



UNIVERSIDADE ESTADUAL DE CAMPINAS
SISTEMA DE BIBLIOTECAS DA UNICAMP
REPOSITÓRIO DA PRODUÇÃO CIENTÍFICA E INTELLECTUAL DA UNICAMP

Versão do arquivo anexado / Version of attached file:

Versão do Editor / Published Version

Mais informações no site da editora / Further information on publisher's website:

<https://www.sciencedirect.com/science/article/pii/S0925838816301438>

DOI: 10.1016/j.jallcom.2016.01.142

Direitos autorais / Publisher's copyright statement:

©2016 by Elsevier. All rights reserved.

DIRETORIA DE TRATAMENTO DA INFORMAÇÃO

Cidade Universitária Zeferino Vaz Barão Geraldo

CEP 13083-970 – Campinas SP

Fone: (19) 3521-6493

<http://www.repositorio.unicamp.br>



On the hardenability of Nb-modified metastable beta Ti-5553 alloy



K.N. Campo, D.R. Andrade, V.C. Opini, M.G. Mello, E.S.N. Lopes, R. Caram*

University of Campinas, School of Mechanical Engineering, Campinas, SP, Brazil

ARTICLE INFO

Article history:

Received 16 October 2015

Received in revised form

8 January 2016

Accepted 19 January 2016

Available online 21 January 2016

Keywords:

Titanium alloys

Aging heat treatment

Hardenability

Hardness

ABSTRACT

Among the commercially available titanium alloys, the metastable β Ti-5553 alloy (Ti–5Al–5V–5Mo–3Cr–0.5Fe wt.%) is an object of great interest because it is employed in aerospace structural applications, primarily in the replacement of steel components. One of the primary advantages of this alloy is its high hardenability, which allows it to retain the β phase at room temperature, even at low cooling rates, thereby allowing the thermoprocessing of thick parts. The aim of this investigation was to evaluate the effect of the replacement of V with Nb on the hardenability of Ti-5553. Based on the molybdenum equivalent criterion, the Nb-modified Ti-5553 alloy was designed to present 12 wt.% of Nb instead of 5 wt.% of V. Samples of both alloys were prepared by melting them in an arc furnace under an inert atmosphere, heat-treated at high temperatures for 12 h and plastic deformed using swage forging. Finally, these samples were solution heat-treated at temperatures above the β -transus followed by cooling at different rates using water quenching, furnace cooling and a modified Jominy end quench test. Characterization was performed by measuring Vickers hardness, X-ray diffraction, and light optical, scanning electron and transmission electron microscopy. The results obtained indicate that metastable β phase can be retained when the cooling rate is higher than 21 °C/s for both alloys. At lower cooling rates, α phase precipitation was observed, but it appeared to be less evident in the Nb-modified Ti-5553, suggesting that the replacement of V with Nb increased the hardenability of the alloy.

© 2016 Elsevier B.V. All rights reserved.

1. Introduction

Metastable β titanium (Ti) alloys have been attracting the attention of various industrial sectors due to their outstanding and versatile properties. Such alloys contain enough β -stabilizing elements to inhibit the martensitic transformation upon quenching, and consequently, the metastable β phase (bcc) can be retained at room temperature. Therefore, their microstructures and mechanical properties can be tailored by controlling the α phase (hcp) precipitation in the metastable β matrix [1,2].

The heat treatment route usually applied to metastable β -Ti alloys to improve their mechanical properties involves the following steps: (i) solution heat treatment in the β -phase field; (ii) cooling to room temperature and (iii) aging at temperatures below the β -transus. From an industrial viewpoint, the major drawback that can arise during this procedure heavily relies on the cooling step, particularly when thick components are involved. This is mainly because of the cooling rate, which must be sufficiently high to avoid

extensive α phase precipitation. The capacity of retaining the β phase after cooling at room temperature varies in each alloy, and this feature is close related to the hardenability of the alloy. According to Luzhnikov, Novikova and Mareev [3], hardenability can be understood as the relationship between the cooling and phase transformation rates. For steels, hardenability involves how deep a section can be strengthened by the martensitic transformation during cooling from the γ -phase field. In the case of metastable β -Ti alloys, the strengthening occurs only later during the aging heat treatment, but it is strongly dependent on the initial microstructure. Therefore, Cotton et al. [4] defined the hardenability of β -Ti alloys in terms of the ability to produce a significant age-hardening response from supersaturated β phase. Accordingly, the thicker the section that can retain the metastable β phase, the higher the hardenability or “quenability” of the alloy.

The Ti-5553 alloy, with chemical composition Ti–5Al–5V–5Mo–3Cr–0.5Fe (wt.%), is a recently developed metastable β alloy that is considered to feature improved hardenability. In this regard, Boyer and Briggs [5] stated that Ti-5553 section sizes up to 152 mm could retain β metastable phase after solution treatment and air-cooling. In addition to its high hardenability, Ti-5553 also presents enhanced mechanical behavior, and

* Corresponding author. Rua Mendeleev, 200, Campinas 13083-860, SP, Brazil.
E-mail address: caram@fem.unicamp.br (R. Caram).

depending on the thermal processing route, the tensile strengths can exceed 1400 MPa [6]. As a result, the Ti-5553 alloy has been an interesting alternative to replace ultrahigh-strength steels and other Ti alloys, such as the Ti-10V-2Fe-3Al, in aircraft applications, leading to substantial weight savings [7].

A previous investigation has shown that the replacement of vanadium (V) with niobium (Nb) in Ti-5553 can lead to improved mechanical strength [8]. However, this replacement possibly changes the kinetics of β phase decomposition (α phase nucleation) and hence the alloy hardenability because it depends directly on the slow diffusers (e.g., Mo, V and Nb) content in the alloy [4]. Therefore, the aim of this investigation is to evaluate the hardenability of Nb-modified Ti-5553 compared to the original Ti-5553 alloy. For this purpose, both alloys were subjected to continuous cooling experiments using a modified Jominy end quench setup, which allows different microstructures to be connected at different cooling rates [3,9–11]. According to Cotton et al. [4], hardenability assessments of commercial β alloys are usually not found in the literature. Thus, the present study also endeavors to provide valuable information to fill this important need.

2. Experimental procedure

Nb-modified Ti-5553 was designed with the goal of total replacement of V with Nb. For this, the molybdenum (Mo) equivalent criterion (wt.%), which is given by the following equation [12], was employed:

$$[\text{Mo}]_{\text{eq}} = \text{Mo} + 0.6\text{V} + 0.44\text{W} + 0.28\text{Nb} + 0.22\text{Ta} + 1.25\text{Cr} + 1.25\text{Ni} + 1.7\text{Co} + 2.5\text{Fe} \quad (1)$$

To maintain the same Mo equivalent as the Ti-5553 alloy, 5 wt.% of V was replaced with 12 wt.% of Nb, resulting in the Ti-12Nb-5Al-5Mo-3Cr-0.5Fe alloy, which will be denoted by Ti-12Nb within this text. As shown in Table 1, the replacement of V with Nb has changed neither the values of the Bo (bond order) and Md (metal d-orbital energy level) parameters nor the electron per atom (e/a) ratio. These parameters are usually applied in the evaluation of phase stability according to the electron approach [13].

Samples of Ti-5553 and Ti-12Nb were prepared by voltaic arc melting in a furnace using a non-consumable tungsten electrode and water-cooled copper crucible under high-purity argon (Ar) atmosphere. Ingots of 70 g were prepared using high-purity elements. To obtain chemical homogeneity, the ingots were remelted and flipped several times. The as-cast ingots were then encapsulated in quartz ampoule with Ar and heat-treated at 1000 °C for 12 h and furnace cooled. These ingots were hot swaged into cylindrical bars with 11.5 mm diameter. These bars were then machined to a 10 mm diameter, and thermocouples were inserted into six drilled holes to acquire the temperature during the modified Jominy end quench test (JQT). Fig. 1a depicts a schematic diagram of the JQT specimen and the respective thermocouple positions (P1 to P6).

The modified JQT [14–18] allows a sample to be cooled at different rates using just one experiment. According to Fig. 1b, cylindrical samples were heated using electromagnetic induction to a

Table 1

Calculated e/a ratio, the Bo and Md parameters and Mo equivalent of the studied alloys.

| Alloy | e/a | Bo | Md | $[\text{Mo}]_{\text{eq}}$ |
|---------|-------|-------|-------|---------------------------|
| Ti-5553 | 4.080 | 2.765 | 2.354 | 13.35 |
| Ti-12Nb | 4.100 | 2.782 | 2.375 | 13.36 |

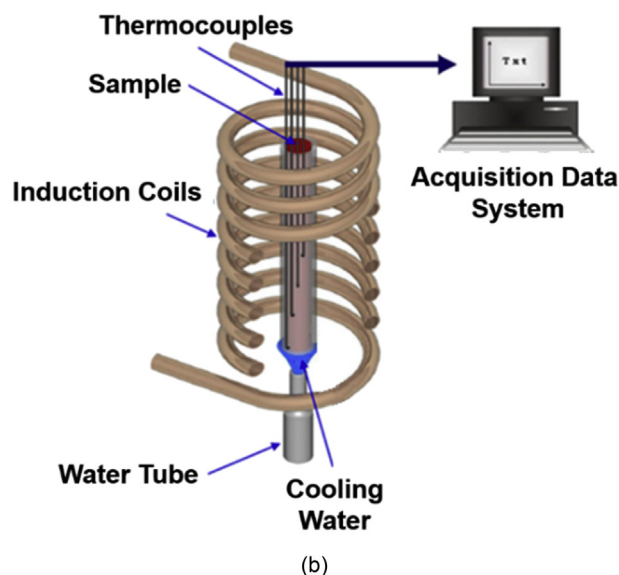
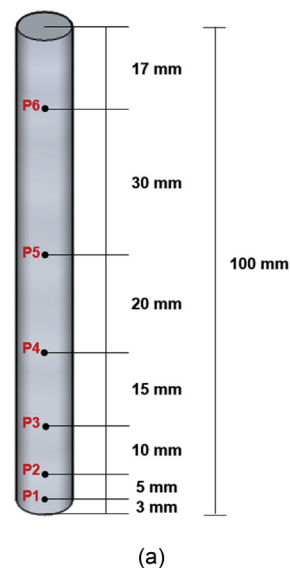


Fig. 1. Schematic illustrations of the modified Jominy end quench test (JQT): (a) specimen and thermocouple positions and (b) experimental setup.

temperature above β -transus (~ 1000 °C). After 15 min in the β -phase field, the samples were quenched from the bottom by a cooling water jet while the temperature was monitored by the type K thermocouples in the six different regions. The cylinder from JQT was sectioned at each of the six thermocouple holes, and the relative cross sections, denoted here as samples P1 to P6, were investigated. To evaluate extreme cooling conditions, disk samples 2 mm in thickness were cut from the swaged bars and solution heat-treated also for 15 min, followed by water quenching (WQ) or furnace cooling (FC).

The chemical composition of the experimental alloys was determined by energy dispersive X-ray fluorescence spectroscopy (Shimadzu EDX7000), whereas the interstitial contents of oxygen (O) and nitrogen (N) were measured in a Leco TC400 analyzer. The resulting samples were subjected to conventional metallographic preparation followed by etching with Kroll's reagent (6 mL of HNO_3 , 3 mL of HF and 91 mL of H_2O). Light optical microscopy was conducted with an Olympus BX60M microscope. Scanning electron

Table 2
Measured chemical composition of the experimental alloys.

| Alloy | Composition (wt.%) | | | | | | | | |
|---------|--------------------|-----------|-----------|-----------|-----------|-----------|------------|---------------|---------------|
| | Ti | Al | V | Mo | Cr | Fe | Nb | O | N |
| Ti-5553 | Balance | 4.5 ± 0.3 | 5.3 ± 0.3 | 4.5 ± 0.4 | 2.7 ± 0.2 | 0.6 ± 0.1 | 0 | 0.197 ± 0.001 | 0.023 ± 0.001 |
| Ti-12Nb | | 5.0 ± 0.1 | 0 | 5.0 ± 0.2 | 3.1 ± 0.1 | 0.6 ± 0.1 | 11.8 ± 0.6 | 0.236 ± 0.001 | 0.016 ± 0.001 |

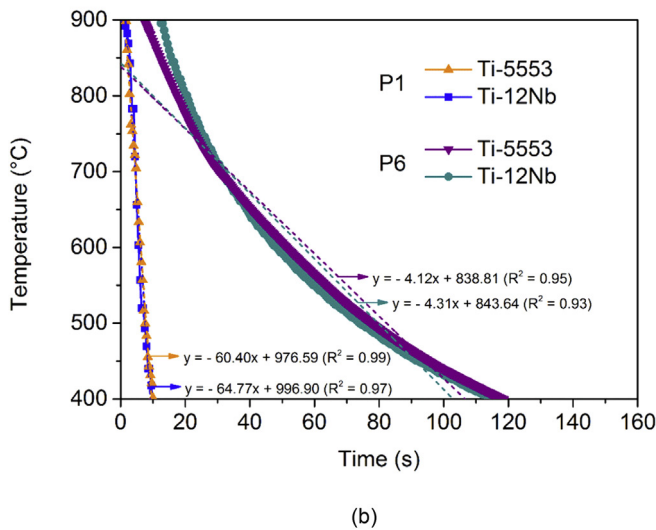
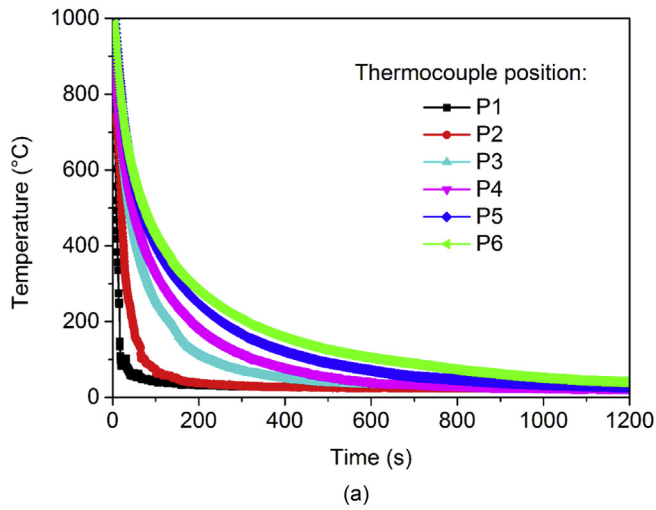


Fig. 2. (a) Cooling curves obtained in the modified JQT for the Ti-12Nb sample. (b) Example of cooling rate estimation by linearly fitting of the cooling curves for the P1 and P6 samples of the Ti-5553 and Ti-12Nb alloys.

Table 3
Estimated cooling rates for each thermocouple position in the JQT specimen and the water-quenched (WQ) and furnace-cooled (FC) samples.

| Sample | Cooling rate (°C/s) |
|--------|---------------------|
| WQ | 261 |
| P1 | 63 |
| P2 | 21 |
| P3 | 10 |
| P4 | 7 |
| P5 | 5 |
| P6 | 4 |
| FC | 0.02 |

Table 4
Mean and standard deviation values of the Vickers hardness of the WQ, JQT and FC samples.

| Sample | Vickers hardness (HV) | |
|--------|-----------------------|---------|
| | Ti-5553 | Ti-12Nb |
| WQ | 327 ± 2 | 303 ± 5 |
| P1 | 272 ± 2 | 274 ± 3 |
| P2 | 264 ± 7 | 258 ± 3 |
| P3 | 275 ± 3 | 272 ± 5 |
| P4 | 279 ± 4 | 276 ± 5 |
| P5 | 283 ± 8 | 278 ± 4 |
| P6 | 292 ± 5 | 280 ± 4 |
| FC | 407 ± 6 | 412 ± 6 |

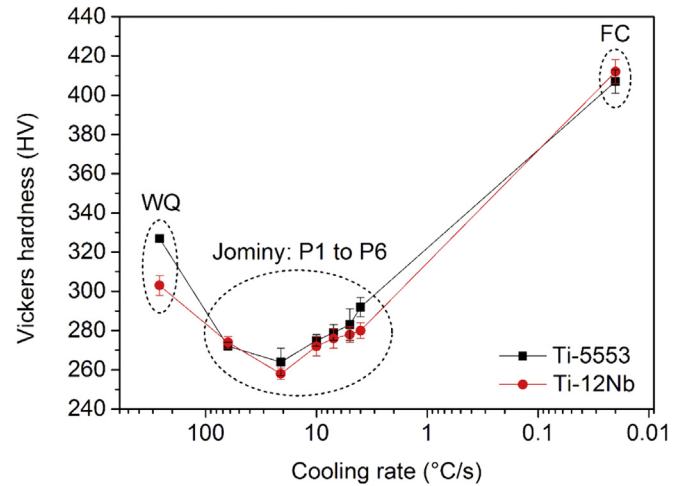


Fig. 3. Vickers hardness as a function of cooling rate for the Ti-5553 and Ti-12Nb alloys.

microscopy (SEM) was conducted using a Zeiss EVO 15. Transmission electron microscopy (TEM) images were obtained from an FEI/Philips CM-200T (200 kV LaB₆) using thin foils prepared in the FEI Helios NanoLab™ 600 DualBeam (FIB/SEM). X-ray diffraction (XRD) (Panalytical X'Pert diffractometer, CuK α radiation, $\lambda = 0.15406$ nm) was employed to index phases. Vickers hardness was measured using a Buehler hardness tester with a load of 1 kgf applied for 15 s. The values of average hardness and standard deviation for each sample were obtained from five measurements.

3. Results and discussion

Table 2 presents the measured chemical compositions of the experimental alloys. The composition measurements reveal that the alloying element contents are in good accordance with the nominal compositions. Moreover, the interstitial levels of O and N are lower than the maximum content normally allowed for Ti alloys established by the ASTM B977 – 13 standard, which are 0.250 and 0.030 for O and N, respectively. This suggests that no contamination occurred during the sample preparation processes and that the

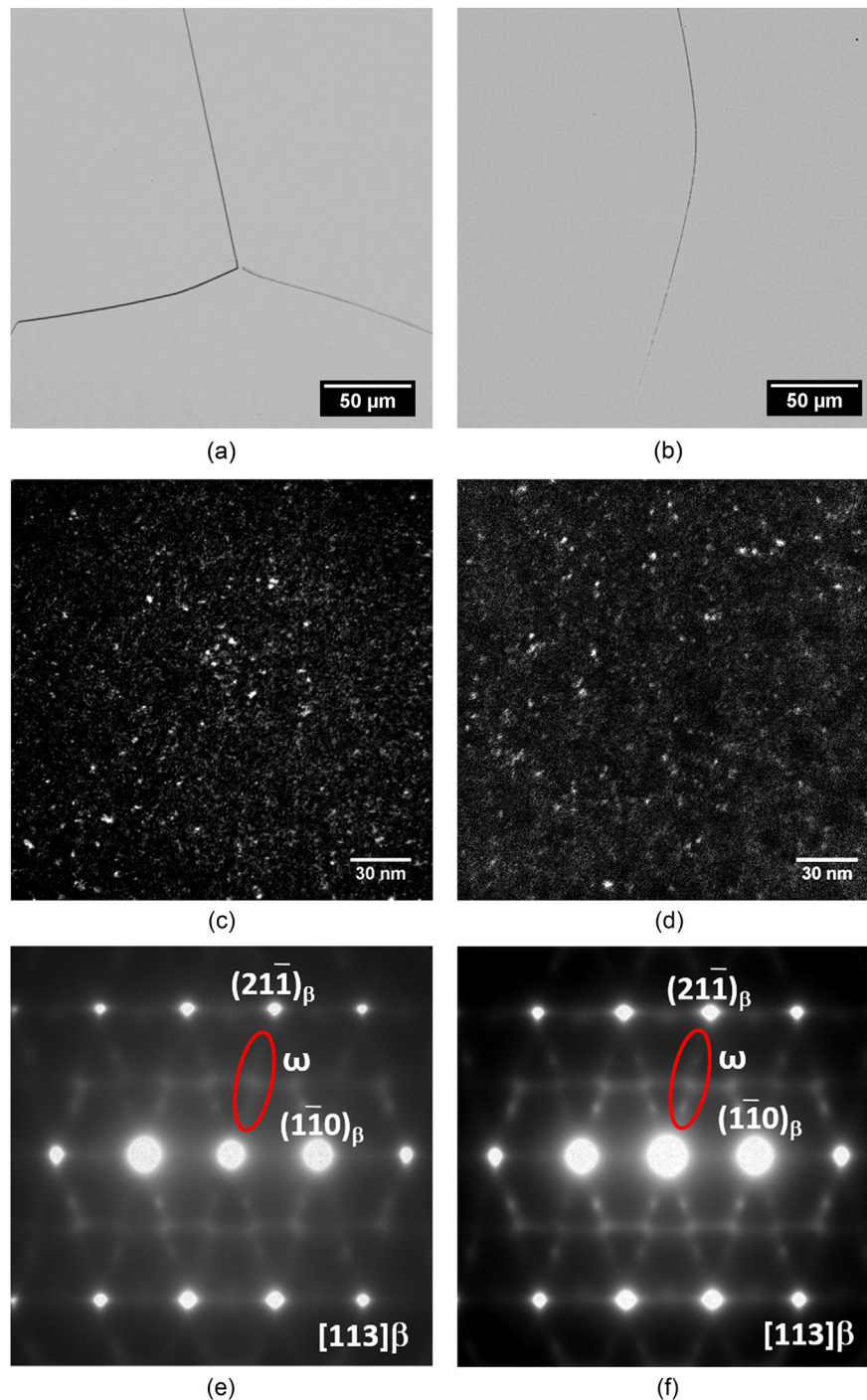


Fig. 4. Light optical micrograph, TEM dark field image and SAD pattern of the microstructures of the water-quenched Ti-5553 (“a”, “c”, “e”) and Ti-12Nb (“b”, “d”, “f”) alloys.

interstitials did not affect the β phase decomposition during the cooling experiments.

Fig. 2a presents the cooling curves registered for each thermocouple positioned along the cylindrical Ti-12Nb sample that was subjected to the modified JQT. It should be noted that no significant difference was observed between the thermal profiles obtained for both alloys that were studied; thus, Fig. 2a is also representative of the Ti-5553 sample. The achieved cooling rates (Table 3) were estimated by linearly fitting the cooling curves in temperatures ranging from 900 to 400 °C as exemplified in Fig. 2b for the P1 and P6 samples of both alloys. This temperature range was selected

because 900 °C is slightly above the β -transus temperature (Ti-5553 alloy [19]), and α phase precipitation is considered improbable at temperatures below 400 °C. From Table 3, it is possible to see that the cooling rate values did not show any expressive difference between the P6 and P4 samples; they ranged from 4 to 7 °C/s, respectively. On the other hand, a significant variation was obtained between the P4 and P1 samples: the cooling rate changed from 7 to 63 °C/s, respectively. Using the same fitting approach, a much higher cooling rate was measured in the WQ sample, 261 °C/s. This value is higher than that reported by Souza et al. [20], which was 200 °C/s. However, these authors worked with thicker samples.

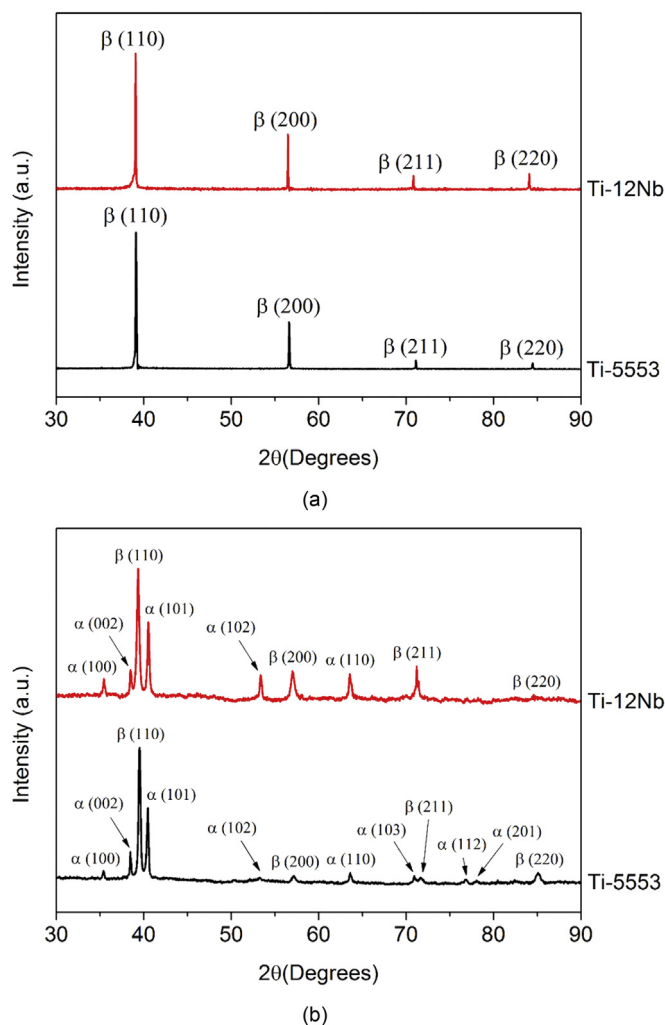


Fig. 5. X-ray diffraction patterns of the Ti-5553 and Ti-12Nb alloys after solution at 1000 °C followed by (a) water quenching and (b) furnace cooling.

Owing to its high cooling rate, the WQ sample could be associated with the surface of the JQT specimen that was directly in contact with the water jet and could not be used because of excessive oxidation. Finally, the cooling rate obtained in the furnace was measured to be approximately 0.02 °C/s. This low rate allows the assumption that equilibrium was reached and hence the age-hardening response of the FC sample is null.

After establishing the cooling rates imposed on the samples, the hardenability of Ti-5553 and Ti-12Nb could be evaluated. Table 4 and Fig. 3 depict the Vickers hardness values as a function of the estimated cooling rates. The hardness profiles are similar for both alloys; they decrease with the cooling rate until reaching a minimum value at a cooling rate of 21 °C/s (P2 samples). From P3 to FC, there is a hardness increase with the decreasing cooling rate. This profile can be explained by the phases resulting from the β decomposition during cooling.

The Ti-5553 and Ti-12Nb microstructures resulting from the water quenching procedure are comparatively depicted in Fig. 4. Under light optical microscopy (Fig. 4a and b), both results show only β phase at room temperature, which is confirmed by the XRD patterns shown in Fig. 5a. However, TEM dark field images (Fig. 4c and d) also allow a highly fine-scale dispersion of ω phase to be identified in both microstructures, which is a result of the athermal transformation from β phase. This observation is based on electron

diffraction evidence, in which the selected area diffraction patterns (SADP) of the $[11\bar{3}]\beta$ zone axis (Fig. 4e and f) show diffuse diffraction spots located at 1/3 and 2/3 of the way between the transmitted beam and the $(2\bar{1}\bar{1})\beta$ phase reflection. The amount of athermal ω phase particles is considerable, and Vickers hardness values of 327 ± 2 HV and 303 ± 5 HV were obtained for Ti-5553 and Ti-12Nb, respectively. Considering these values, the difference between them can be explained by the solid solution effect of the alloying elements in the β phase of these alloys. However, these dissimilar hardness values can also be attributed to a possible difference in the amount of ω phase. It is well known that adding β -stabilizers suppresses the athermal $\beta \rightarrow \omega$ transformation [21]. Although both alloys studied here present the same Mo equivalent, the replacement of V with Nb may have hindered athermal ω phase precipitation and, therefore, its amount is probably lower in the Ti-12Nb alloy, which explains its lower hardness. Nonetheless, quantitative determination of athermal ω phase is not a simple task, and to the best of the authors' knowledge, no related work has been published.

As already mentioned, a decrease in hardness with decreasing cooling rate was observed for the P1 and P2 samples (Fig. 3). Microstructure evaluation of these samples using light optical microscopy and X-ray diffraction yielded analogous results in the WQ samples (Figs. 4a, b and 5a). In this case, despite the lower cooling rates, no evidence of α precipitation was found. Fig. 6 presents the TEM analyses of the P2 sample for the Ti-5553 and Ti-12Nb alloys. Again, the presence of athermal ω phase in the β phase matrix can be identified. From these results, it is possible to conclude that the microstructures of both alloys are formed only by $\beta + \omega$ in cooling rates ranging from 261 to 21 °C/s. Although they present the same phases, the hardness values are dissimilar, suggesting that the amount of athermal ω phase is reduced with the decreased cooling rates. It is interesting to note that, in contrast to the WQ condition, the P1 and P2 samples of the Ti-5553 and Ti-12Nb alloys exhibit similar hardness values. This was interpreted as evidence that the amount of ω phase affected the hardness values in the WQ samples more significantly than the solid solution.

The hardness values begin to increase from P3 samples, indicating the onset of α phase precipitation. According to the XRD analyses (Fig. 7), it was possible to identify α phase in the P3 sample of Ti-5553, as demonstrated by the diffraction peak near 35°, which is related to the (100) plane. Nevertheless, α phase identification was possible only in the P5 sample of Ti-12Nb. This implies that either α phase precipitation occurred only in P5, or the volume fraction of α phase in P3 and P4 was too small to be detectable by the XRD technique. To obtain a more detailed characterization, the P3 sample of the Ti-12Nb alloy was examined by TEM (Fig. 8). The TEM dark field image (Fig. 8a) clearly shows discrete needles of α phase with lengths of ~100 nm. However, owing to its low volume fraction, the SADP (Fig. 8b) presents weak diffuse spots of the $\{10\bar{1}0\}$ family of planes.

Fig. 9 depicts backscattered SEM images of samples P3–P6 of the Ti-5553 and Ti-12Nb alloys. In this case, etched areas in the β grains are cavities corresponding to the α phase, which was selectively corroded. It should be noted that α phase precipitates could be observed only in etched samples; its low volume probably did not allow a sufficient backscattered contrast to be obtained in non-etched samples. By comparing the microstructures, it is clear that the Ti-5553 samples show a more intense α phase precipitation than those of Ti-12Nb. Sample P3 of Ti-12Nb seems to present a fully β microstructure. However, the previous TEM analyses (Fig. 8) confirmed α phase precipitation. With the decreased cooling rate (P4 and P5), scarce α phase precipitation evidence in the β phase matrix appears in some regions. A strong indication of α phase is observed only in sample P6, but it seems to be a nonhomogeneous

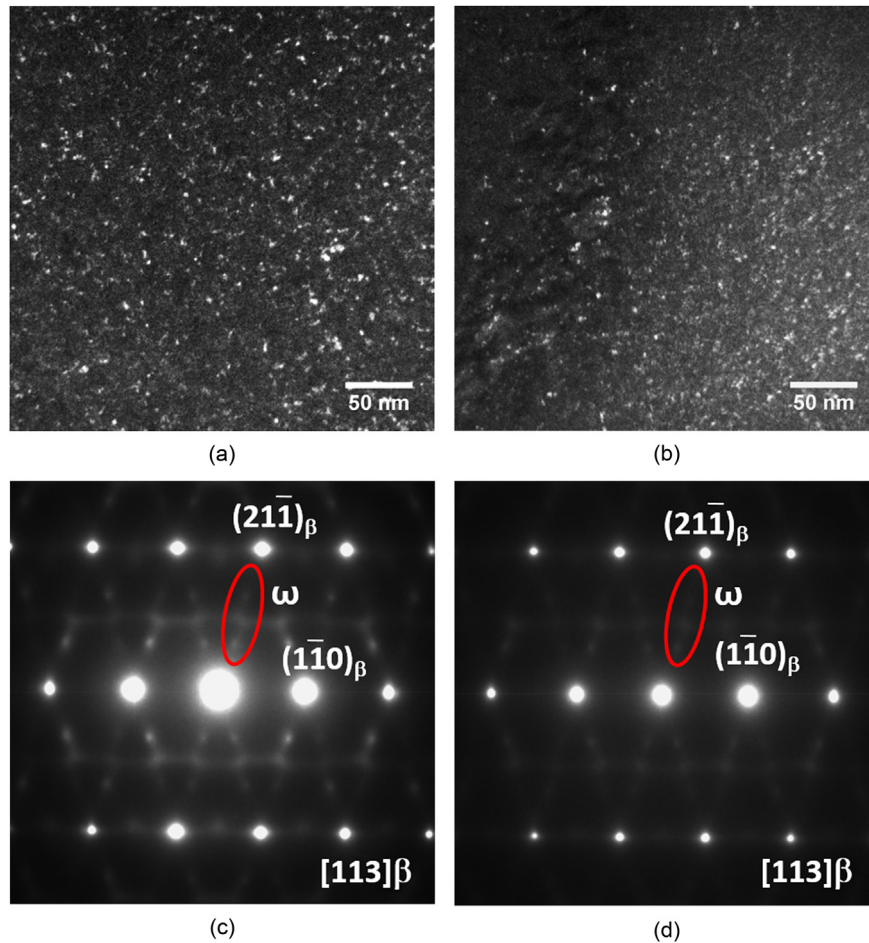


Fig. 6. TEM dark field image and SAD pattern of the microstructures of the P2 position of the Ti-5553 (“a”, “c”) and Ti-12Nb (“b”, “d”) alloys.

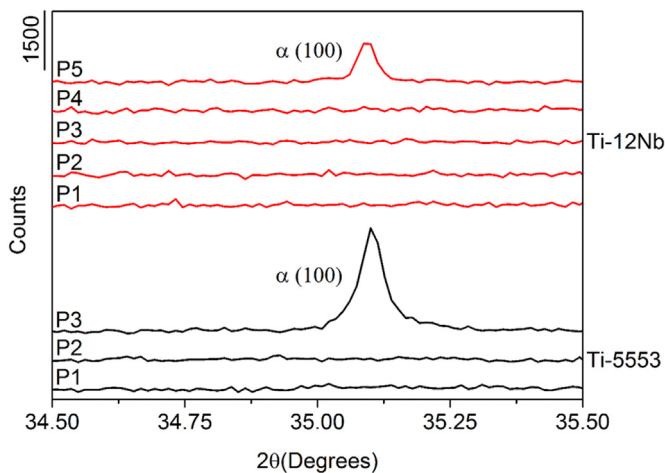


Fig. 7. X-ray diffraction patterns of the Ti-5553 and Ti-12Nb alloys showing the onset of α phase precipitation.

precipitation. Nonetheless, it is believed that this must be an etching artifact. Despite the difference in α phase content in the microstructures of the alloys, no significant contrast is observed in the hardness values for samples P3 to P5. This probably is related to some solid solution effect caused by the relatively large Nb content

in Ti-12Nb.

Whereas the solution heat treatment followed by water quenching produced a microstructure formed by $\beta + \omega$, the furnace cooling led to total decomposition of the β phase and nucleation of α precipitates with high crystallographic ordering in the β grains (Figs. 5b and 10). The microstructures shown in Fig. 10 reveal that the replacement of V with Nb led to a more refined structure, although some coarse α phase needles coexist, mainly in the grain boundaries. Nonetheless, this microstructural refinement did not affect the Vickers hardness because both alloys in the FC condition presented average hardness of approximately 410 HV (Table 4). This value is already high, and it is obvious that no strengthening is expected in a subsequent aging treatment because there is no driving force for an expressive microstructural change.

In this study, the achieved critical quench rate was 21 °C/s for both alloys. Based on the obtained results, diffusional α phase formation is avoided whether the applied cooling rate is higher than 21 °C/s. On the other hand, cooling rates lower than 10 °C/s allowed α phase precipitation, which appears to be more intense in the Ti-5553 alloy. This suggests that the replacement of V with Nb reduces the β phase decomposition kinetics. One possible reason for this behavior is the larger Nb content, which increases the complexity of the solute redistribution during the α phase formation because more atoms are involved. In addition, the slightly lower diffusion rate of Nb in Ti compared to V [22–24] may have also contributed to lowering α phase precipitation. The combination of these effects is believed to explain the improved hardenability or “quenchability”

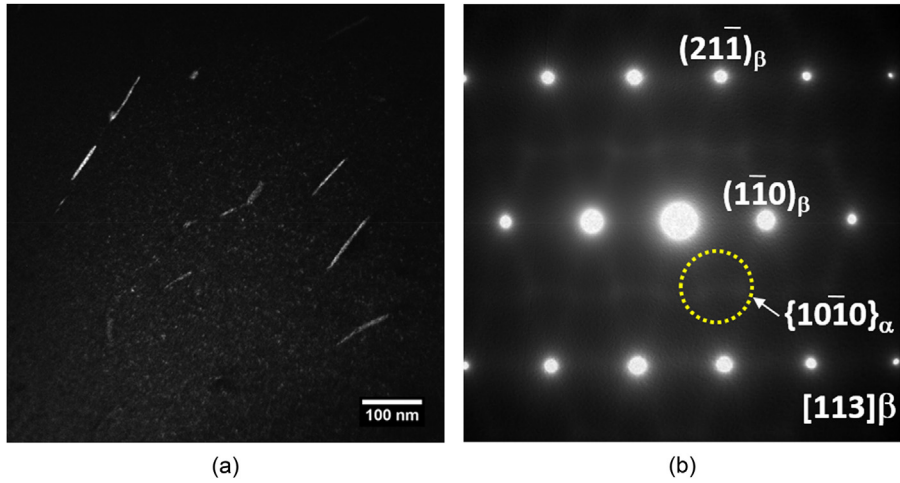


Fig. 8. (a) TEM dark field image from α phase reflection spots (circle). (b) SAD pattern of the microstructure of the P3 position of the Ti–12Nb alloy.

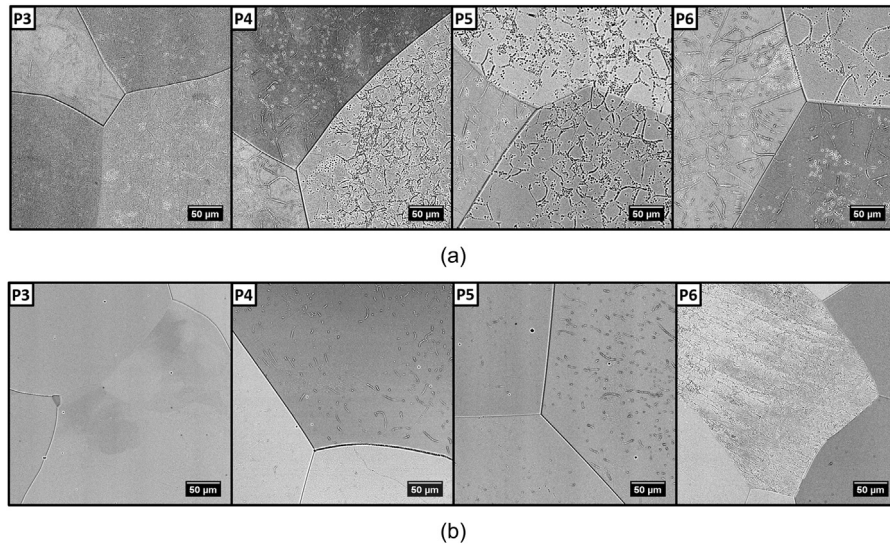


Fig. 9. Backscattered SEM images of samples P3 to P6 for the (a) Ti-5553 and (b) Ti–12Nb alloys.

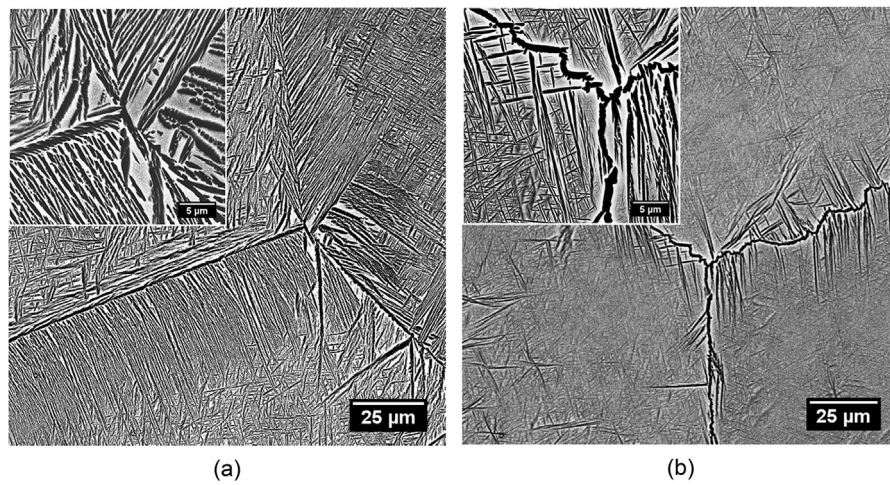


Fig. 10. Backscattered SEM images of the FC samples for the (a) Ti-5553 and (b) Ti–12Nb alloys.

of the Ti–12Nb alloy.

A final remark regards the effect of the V replacement with Nb on the β -transus temperature of the Ti–12Nb alloy compared to the Ti-5553 alloy. Cotton et al. [4] stated that the β -stabilizer content could reduce the β -transus temperature to a point at which the ability to subsequently age hardening is diminished by the slow diffusion rates at lower temperatures. Therefore, the β -transus temperatures of the studied alloys were determined. For this, an iterative process was carried out. A sample was maintained at a certain temperature for 15 min followed by rapid quenching; if the presence of α phase was identified, the process was performed again at a higher temperature. This process was repeated until the β -transus was found three times for each alloy to consider experimental errors. Following this approach, the β -transus temperature for the Ti-5553 alloy was found to be 859 ± 2 °C, which is near that reported by Fanning [19], 856 °C. The β -transus temperature obtained for the Ti–12Nb alloy was 851 ± 1 °C. Based on these values, this slight reduction cannot be considered to be detrimental to the subsequent aging treatment.

4. Conclusions

The following conclusions can be drawn from this investigation:

- Ti-5553 and Ti–12Nb presented similar Vickers hardness profiles as a function of cooling rate. The hardness values decreased with the cooling rate until a minimum value at a cooling rate of 21 °C/s. The variation of the cooling rate from 261 to 21 °C/s resulted in microstructures with β and ω phases. The decreased hardness in this range was interpreted to be a reduction of athermal ω phase. Cooling rates lower than 10 °C/s allowed the α phase precipitation for both alloys. Consequently, there was an increase in hardness with decreasing cooling rate from this point.
- Although both alloys presented the α phase precipitation at cooling rates lower than 10 °C/s, it appeared to be less intense in the Ti–12Nb alloy. This suggests that the replacement of V with Nb reduced the β phase decomposition kinetics and hence enhanced the hardenability of the alloy. It seems reasonable to attribute this behavior to the higher alloying element content in the Ti–12Nb and the more sluggish diffusion of Nb.
- The replacement of V with Nb caused the β -transus temperature to drop. The experimental results showed that this temperature is 859 °C for Ti-5553, whereas it is 851 °C for Ti–12Nb.

Acknowledgments

The authors gratefully acknowledge the Brazilian research funding agencies FAPESP (São Paulo Research Foundation) Grant # 2012/11742-5 and CNPq (National Council for Scientific and Technological Development) Grant # 484379/2012-7 for their financial support. We are also indebted to CBMM Co. for supplying Nb and to Prof. Hamish L. Fraser for providing access to the FIB/TEM facilities in the CEMAS/Ohio State University.

References

- [1] G. Lütjering, J.C. Williams, Titanium, Springer, Berlin, 2003, <http://dx.doi.org/10.1007/978-3-540-73036-1>.

- [2] C. Leyens, M. Peters, Titanium and Titanium Alloys – Fundamentals and Applications, Wiley-VCH, Köln, 2004, <http://dx.doi.org/10.1002/3527608117.fmatter>.
- [3] L.P. Luzhnikov, V.M. Novikova, A.P. Mareev, Hardenability of industrial titanium alloys, Met. Sci. Heat. Treat. 7 (1965) 335–338, <http://dx.doi.org/10.1007/BF00649026>.
- [4] J.D. Cotton, R.D. Briggs, R.R. Boyer, S. Tamirisakandala, P. Russo, N. Shchetnikov, J.C. Fanning, State of art in beta titanium alloys for airframe applications, JOM-J Min. Met. Mat. S 67 (2015) 1281–1303, <http://dx.doi.org/10.1007/s11837-015-1442-4>.
- [5] R.R. Boyer, R.D. Briggs, The use of β titanium alloys in the aerospace industry, J. Mater Eng. Perform. 14 (2005) 681–685, <http://dx.doi.org/10.1361/105994905X75448>.
- [6] N. Clément, A. Lenain, P.J. Jacques, Mechanical property optimization via microstructural control of new metastable beta titanium alloys, JOM-J Min. Met. Mat. S 59 (2007) 50–53, <http://dx.doi.org/10.1007/s11837-007-0010-y>.
- [7] R.R. Boyer, Attributes, characteristics, and applications of titanium and its alloys, JOM-J Min. Met. Mat. S 62 (2010) 21–24, <http://dx.doi.org/10.1007/s11837-010-0071-1>.
- [8] Opini VC, Salvador CAF, Lopes ESN, Chaves RR, Caram R, α phase precipitation and mechanical properties of Nb-modified Ti-5553 alloy, (to be published).
- [9] C.F. Hickey, P.J. Fopiano, Some observations on the hardenability of Ti-6Al-6V-2Sn, Metall. Trans. B 1 (1970) 1775–1777, <http://dx.doi.org/10.1007/BF02642031>.
- [10] K. Frkáňová, J. Lapin, Relationship between microstructure and cooling rate in air-hardenable TiAl-based alloy, in: Metal 2012: 24th International Conference on Metallurgy and Materials, 2012, 23–25.5. 2012, Brno, Czech Republic, EU.
- [11] A.Z. Yazdi, S.A. Sajjadi, S.M. Zabarjad, S.M.M. Nezhad, Prediction of hardness at different points of Jominy specimen using quench factor analysis method, J. Mater Process Tech. 199 (2008) 124–129, <http://dx.doi.org/10.1016/j.jmatprotec.2007.08.035>.
- [12] I. Weiss, S.L. Semiantin, Thermomechanical processing of alpha titanium alloy – an overview, Mater Sci. Eng. A 263 (1999) 243–256, [http://dx.doi.org/10.1016/S0921-5093\(98\)01155-1](http://dx.doi.org/10.1016/S0921-5093(98)01155-1).
- [13] M. Abdel-Hady, K. Hinoshita, M. Morinaga, General approach to phase stability and elastic properties of β -type Ti-alloys using electronic parameters, Scr. Mater. 55 (2006) 477–480, <http://dx.doi.org/10.1016/j.scriptamat.2006.04.022>.
- [14] T. Ahmed, H.J. Rack, Phase transformations during cooling in $\alpha + \beta$ titanium alloys, Mat. Sci. Eng. A 243 (1998) 206–211, [http://dx.doi.org/10.1016/S0921-5093\(97\)00802-2](http://dx.doi.org/10.1016/S0921-5093(97)00802-2).
- [15] C.R.M. Afonso, G.T. Aleixo, A.J. Ramirez, R. Caram, Influence of cooling rate on microstructure of Ti-Nb alloy for orthopedic implants, Mat. Sci. Eng. C 27 (2007) 908–913, <http://dx.doi.org/10.1016/j.msec.2006.11.001>.
- [16] S.A. Souza, C.R.M. Afonso, P.L. Ferrandini, A.A. Coelho, R. Caram, Effect of cooling rate on Ti-Cu eutectoid alloy microstructure, Mat. Sci. Eng. C 29 (2009) 1023–1028, <http://dx.doi.org/10.1016/j.msec.2008.09.007>.
- [17] G.T. Aleixo, E.S.N. Lopes, R. Contieri, A. Cremasco, C.R.M. Afonso, R. Caram, Effects of cooling rate and Sn addition on the microstructure of Ti-Nb-Sn alloys, Solid State Phenom. 172–174 (2011) 190–195, 10.4028/www.scientific.net/SSP.172-174.190.
- [18] R.J. Contieri, E.S.N. Lopes, R. Caram, A. Devaraj, S. Nag, R. Banerjee, Effects of cooling rate on the microstructure and solute partitioning in near eutectoid Ti-Cu alloys, Philos. Mag. 94 (2014) 2350–2371, <http://dx.doi.org/10.1080/14786435.2014.913113>.
- [19] J.C. Fanning, Properties of TIMETAL 555 (Ti-5Al-5Mo-5V-3Cr-0.6Fe), J. Mater Eng. Perf. 14 (2005) 788–791, <http://dx.doi.org/10.1361/105994905X75628>.
- [20] S.A. Souza, R.B. Manicardi, P.L. Ferrandini, C.R.M. Afonso, A.J. Ramirez, R. Caram, Effect of the addition of Ta on microstructure and properties of Ti-Nb alloys, J. Alloy Compd. 504 (2010) 330–340, <http://dx.doi.org/10.1016/j.jallcom.2010.05.134>.
- [21] T.W. Duerig, J.C. Williams, in: R.R. Boyer, H.W. Rosenberg (Eds.), β Titanium Alloys in the 1980's, American Institute of Mining, Metallurgical, and Petroleum Engineers, Inc., New York, 1984.
- [22] G.B. Gibbs, D. Graham, D.H. Tomlin, Diffusion in titanium and titanium – niobium alloys, Philos. Mag. 8 (1963) 1269–1282, <http://dx.doi.org/10.1080/14786436308207292>.
- [23] J.F. Murdock, C.J. McHargue, Self-diffusion in body-centered cubic titanium-vanadium alloys, Acta Metall. 16 (1968) 493–500, [http://dx.doi.org/10.1016/0001-6160\(68\)90123-5](http://dx.doi.org/10.1016/0001-6160(68)90123-5).
- [24] G. Neumann, C. Tuijin, Self-diffusion and Impurity Diffusion in Pure Metals: Handbook of Experimental Data, Elsevier Science, London, 2008.